UDC 623.451.7:629.7.016

Zamyshlyaev A. A., Shmygin A. N., Donovskiy D. E.

Research aimed at expanding the range of permissible application modes of aircraft equipment

The article shows a cycle of design-theoretical and laboratory work, which provided opportunities to significantly expand the application mode of aviation equipment without additional flight tests. The work was carried out in four stages: determination of impact air pressure and static pressure receiving coefficients, development of computer programs, laboratory bench-test at the air pressure receiving system (APRS) and APRS parameters computational determination in the whole range of application modes.

Keywords: receiving coefficients, range of application modes, pressure receiving system, quasi-one-dimensional flow.

As a rule, aeronautical products are used within the whole range of permissible application modes (RPAM) set in the terms of reference based on the analysis of operation of their systems and devices following flight tests (FT) depending on the flight mode. In some aeronautical products, one of the systems with its characteristics mostly determining the RPAM extent is air pressure receiving system (APRS).

APRS consists of pressure intakes (PI) and pressure measuring instruments (PMI) connected by ducting. The PI are located on the outer surface of the product enclosure and PMI – inside the product; the ducting length is much greater than their diameter. Fig. 1, a shows the APRS in a simplified form. Receipt of static pressure, $P_{ст}$ (С), is done by means of the PI within its backside intake and of dynamic pressure, $P_{д}$ (Д), – by means of its intake on a front side; the intakes are connected with the PMI by ducting. Main characteristics of the PI are the ram air pressure receiving factor $K = q_{вн}/q$, and the static pressure receiving factor $Ky = P_{ст}/P$, where q and P are values of the ram and static pressure of the airstream. The K and Ky factors describe the differences between pressures $P_{ст}$ and $P_{д}$ received by means of the PI and the pressure in the undisturbed stream. These differences are due to the peculiarities of streamlining of the product outer contours by ram air stream, as well as structural parameters of the PI and ducting system.

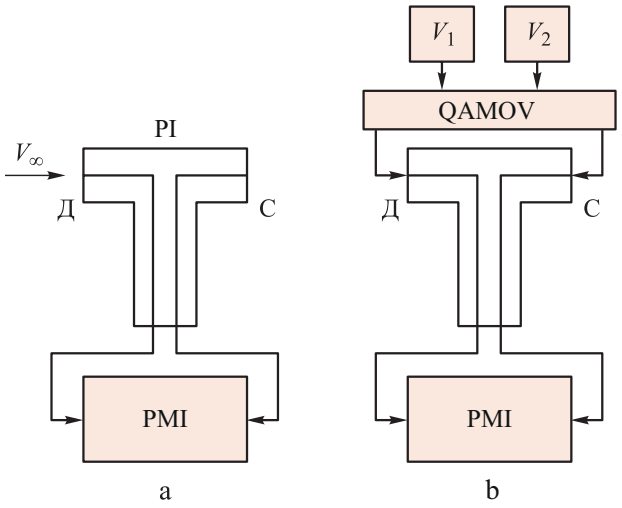

Fig. 1. Scheme of APRS (a) and APRS laboratory bench (b)

Initially, the PI inlets are closed, $P_{ст}$ and $P_{д}$ are not received, APRS is air-tight. Opening of the inlets is done at the set point during the product flight. Following non-steady processes related to pressure equalization in the $P_{ст}$ and $P_{д}$ inlet channels, as well as in the APRS ducting, when the difference $q_{вн} = P_{д} - P_{ст}$ reaches a defined value, PMI actuation takes place.

The following condition shall be fulfilled: the PMI actuation time counted from the time of the PI inlets opening should not exceed the set value within the whole RPAM. Fulfilling this requirement shall be confirmed based on the FT results.

However, considering the limited scope of product FT, inability (in certain cases) to test the products under the marginal conditions, confirmation based on the FT results is not always possible. Particularly, it relates to the requirement of the PMI actuation time within the whole RPAM indicated in the field performance specification.

© Zamyshlyaev A. A., Shmygin A. N., Donovskiy D. E., 2016

Finally, this can significantly limit the product's RPAM scope; to remove the limitations, additional FT are normally required.

The aim of this paper is to carry out research to extend the RPAM of an aeronautical product without additional FT.

During the work, it was required to address the main task and to confirm fulfilment of the requirements to the PMI actuation time within the RPAM sub-area, in which no FT were performed.

This work was done in several stages (Fig. 2).

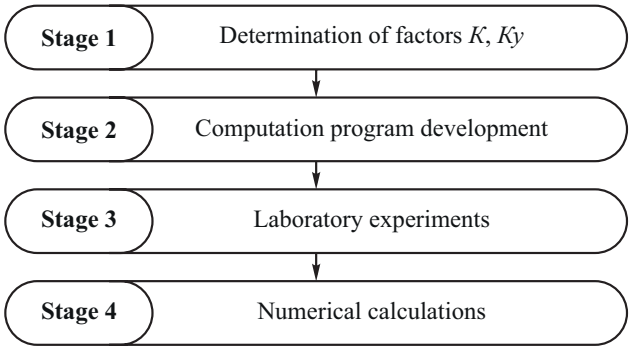

Fig. 2. Work performance procedure

Stage 1 implied determination of ram air pressure receipt factor K and static pressure receipt factor *Ky* in the sub-area not addressed during the FT following the analysis of characteristics of an aeronautical products with similar (close) aerodynamic contours and PI arrangement on the body. Fig. 3 shows the relations of relative factors $K' = K/K_{max}$ (solid line) and $Ky' = Ky/Ky_{max}$ (dot line) vs. relative number $M' = M/M_{max}$, which were obtained at stage 1. The results obtained based on estimated and theoretical studies are shown in Fig. 3 in a dimensionless form $K' = K/K_{max}$, $Ky' = Ky/Ky_{max}$, $M' = M/M_{max}$.

At stage 2, an *SPD* computation program was developed to estimate the transit processes inside the APRS and determine its characteristics based on initial and boundary conditions, as well as the APRS structural parameters: ducting length and radius, size of free (measuring) volumes of the PMI.

The indicated computation program covers simplified representation of the APRS, i.e.

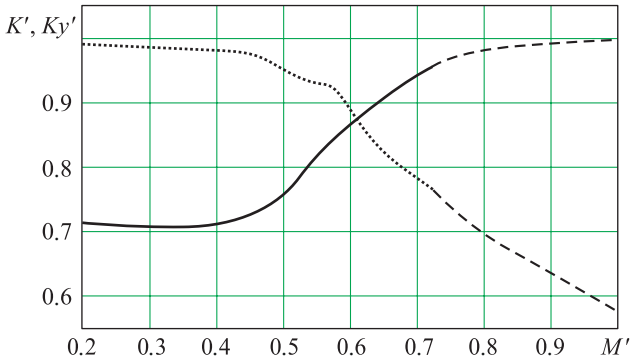

Fig. 3. Dependences of factors K' and Ky'

non-standard quasi-one-dimensional stream of the compressed perfect gas in a straight duct with uniform cross-section, length L, and radius h (L is assumed to be significantly greater than h), ending with a spherical volume (vessel) with the radius R, simulating the PMI free volume.

The task set in this form presupposes consistency of physical parameters at the duct section, as well as prompt change of parameters in each ducting section due to the wall action.

At the initial moment t_0, initial values of pressure P_0, density ρ_0, and velocity U_0, are set in the duct and vessel, boundary values of pressure, P_1 (at this, $P_1 \neq P_0$) and density, ρ_1 – at the duct inlet boundary, and zero value of the gas velocity – on the vessel wall.

Dimensionless equations of movement, mass and energy conservation considering corrections for resistance of the ducting and vessel walls [1], jointly with the thermodynamic equation of gas state are written as follows:

$$\frac{\partial U}{\partial t} + U\frac{\partial U}{\partial x} = \frac{1}{\rho}\frac{\partial U}{\partial x} - \frac{C_f U|U|}{h}, \quad (1)$$

$$\frac{\partial \rho}{\partial t} + \rho\frac{\partial U}{\partial x} + U\frac{\partial \rho}{\partial x} + \frac{\rho U}{S}\frac{\partial S}{\partial x} = 0, \quad (2)$$

$$\frac{\partial e}{\partial t} + U\frac{\partial e}{\partial x} = -P\left[U\frac{\partial}{\partial x}\left(\frac{1}{\rho}\right) + \frac{\partial}{\partial t}\left(\frac{1}{\rho}\right)\right] + \frac{C_f U^2|U|}{h}, \quad (3)$$

$$P = (\gamma - 1)\rho e. \quad (4)$$

Here, U – velocity;

ρ – density;

C_f – permanent factor;

e – specific internal energy;

P – pressure;

γ – adiabatic exponent.

Formulas for change of the cross-section area in the ducting and vessel are taken from the paper [2]: $S = \pi h^2$ at $x \le L$, $S = 2\pi(x - L)^2$ at $x \ge L + h$, $S = \pi(h^2 + (x - L)^2)$ at $L < x < L + h$.

Initial conditions are set as follows:

$$P|_{t=0} = P_0,\ \rho|_{t=0} = \rho_0,\ U|_{t=0} = U_0$$

$$\text{at } 0 < x < L + R,$$

and boundary conditions have the form:

$$P|_{x=0} = P_1,\ \rho|_{x=0} = \rho_1,\ U|_{x=L+R} = 0,$$

where $U|_{x=L+R} = 0$ – value of gas velocity on the vessel wall.

A "splitting method" was applied for numerical solution of equations (1)–(4) jointly with boundary and initial conditions [3]. The method is based on the concept that the whole time interval is split into two semi-intervals: the first semi-interval uses an explicit leap-frog scheme, where the coordinates of the cross-section area and velocity are calculated in the whole grid nodes, while the pressure, density and specific inner energy – in half grid nodes [4]. The second semi-interval uses upwind one-sided differences [5]. Split equation analogues (1)–(4) with $n + 1/2$ and $n + 1$ intervals are written as follows:

$$U_i^{n+1/2} = U_i^n - \frac{\Delta t}{\rho_{i+1/2}^n}\frac{P_{i+1/2}^n + q_{i+1/2}^n - P_{i-1/2}^n - P_{i-1/2}^n}{\Delta x} - \frac{C_f U_i^n \left|U_i^n\right| \Delta t}{h};$$

$$\rho_{i+1/2}^{n+1/2} = \frac{\rho_{i+1/2}^n}{1 + \frac{\left(U_{i+1}^n - U_i^n\right)\Delta t}{\Delta x} + \frac{\left(U_{i+1}^n + U_i^n\right)\left(S_{i+1}^n - S_i^n\right)\Delta t}{\left(S_{i+1}^n + S_i^n\right)\Delta x}};$$

$$e_{i+1/2}^{n+1/2} = e_{i+1/2}^n - \frac{P_{i+1/2}^n + q_{i+1/2}^{n+1/2}}{\rho_{i+1/2}^{n+1/2}} + \frac{P_{i+1/2}^n + q_{i+1/2}^{n+1/2}}{\rho_{i+1/2}^n} + \frac{C_f \frac{1}{4}\left(U_{i+1}^{n+1/2} + U_{i+1}^n\right)^2 \left|\frac{1}{2}\left(U_i^{n+1/2} + U_i^{n+1/2}\right)\right| \Delta t}{h};$$

$$P_{i+1/2}^{n+1/2} = (\gamma - 1)\rho_{i+1/2}^{n+1/2} e_{i+1/2}^{n+1/2};$$

$$U_i^{n+1} = U_i^{n+1/2} - U_i^{n+1/2}\begin{cases}\left(U_{i+1}^{n+1/2} - U_i^{n+1/2}\right)\frac{\Delta t}{\Delta x}, \text{ if } U_i^{n+1/2} < 0, \\ \left(U_i^{n+1/2} - U_{i-1}^{n+1/2}\right)\frac{\Delta t}{\Delta x}, \text{ if } U_i^{n+1/2} > 0;\end{cases}$$

$$\rho_{i+1/2}^{n+1} = \rho_{i+1/2}^{n+1/2} - U_{i+1/2}^{n+1/2}\begin{cases}\left(\rho_{i+3/2}^{n+1/2} - \rho_{i+1/2}^{n+1/2}\right)\frac{\Delta t}{\Delta x}, \text{ if } U_i^{n+1/2} < 0, \\ \left(\rho_{i+1/2}^{n+1/2} - \rho_{i-1/2}^{n+1/2}\right)\frac{\Delta t}{\Delta x}, \text{ if } U_i^{n+1/2} > 0;\end{cases}$$

$$e_{i+1/2}^{n+1} = e_{i+1/2}^{n+1/2} - U_{i+1/2}^{n+1/2} \times \begin{cases}\left(e_{i+3/2}^{n+1/2} - e_{i+1/2}^{n+1/2}\right)\frac{\Delta t}{\Delta x} - \left(\frac{P_{i+1/2}^{n+1/2} + q_{i+1/2}^{n+1/2}}{\rho_{i+3/2}^{n+1/2}} - \frac{P_{i+1/2}^{n+1/2} + q_{i+1/2}^{n+1/2}}{\rho_{i+1/2}^{n+1/2}}\right)\frac{\Delta t}{\Delta x}, \\ \text{if } U_i^{n+1/2} < 0, \\ \left(e_{i+1/2}^{n+1/2} - e_{i-1/2}^{n+1/2}\right)\frac{\Delta t}{\Delta x} - \left(\frac{P_{i+1/2}^{n+1/2} + q_{i+1/2}^{n+1/2}}{\rho_{i+1/2}^{n+1/2}} - \frac{P_{i+1/2}^{n+1/2} + q_{i+1/2}^{n+1/2}}{\rho_{i-1/2}^{n+1/2}}\right)\frac{\Delta t}{\Delta x}, \\ \text{if } U_i^{n+1/2} > 0;\end{cases} - \frac{P_{i+1/2}^{n+1/2} + q_{i+1/2}^{n+1/2}}{\rho_{i+1/2}^{n+1}} + \frac{P_{i+1/2}^{n+1/2} + q_{i+1/2}^{n+1/2}}{\rho_{i+1/2}^{n+1/2}};$$

$$P_{i+1/2}^{n+1} = (\gamma - 1)\rho_{i+1/2}^{n+1} e_{i+1/2}^{n+1}.$$

Here: $C_{i+1/2}^{n+1/2} = \gamma\frac{P_{i+1/2}^{n+1/2}}{\rho_{i+1/2}^{n+1/2}}$; $U_{i+1/2}^{n+1/2} = \frac{U_{i+1}^{n+1/2} + U_i^{n+1/2}}{2}$;

$$q_{i+1/2}^{n+1/2} = q_l C_{i+1/2}^n \left(\rho_{i+1/2}^{n+1/2} - \rho_{i+1/2}^n\right) + q_q \rho_{i+1/2}^n \left(U_{i+1}^n - U_{i+1}^n\right)^2.$$

Initial conditions: $P_i^0 = P_1$, $\rho_i^0 = \rho_1$, $U_i^0 = U_1$ $(0 < i < N)$.

Boundary conditions: $P_{1/2}^{n+1/2;n+1} = P_2$, $\rho_{1/2}^{n+1/2;n+1} = \rho_2$; $U_N^{n+1/2;n+1} = 0$.

To check reliability of the obtained results using the above mentioned computation program, there was a comparison of the numerical calculation results and exact analytical solutions, particularly, the task on discontinuity breakup, and the task on shock wave reflection from a rigid wall [6].

Comparison results are given in Figs. 4, 5. Initial conditions on the parameters distribution are set as follows: for the task on discontinuity breakup within the interval of $x = 0…0.5$ (left) – $P_l = 1$, $\rho_l = 1$, $U_l = 0$, $x = 0.5…1$ (right) – $P_r = 0.1$ $\rho_r = 0.125$, $U_r = 0$, for the task on shock wave reflection from a rigid wall within the interval $x = 0…2.5 – P_i = 0.5$, $\rho_l = 1$, $U_l = 2.8026$ (left), $x = 2.5…3 – P_r = 2.5$, $\rho_r = 1$, $U_r = 0$ (right), with $x = 3$ the rigid wall condition was set.

Figs. 4, 5 show acceptable correlation of calculation results using the SPD program and exact analytical solutions.

At stage 3, the laboratory bench of real APRS structure was developed including ducting, PMI, PI, and tests for all the required RPAM were conducted. Pressures $P_{ст}$ and $P_{д}$ in the RPAM bench structure were set using the air pressure tanks with the volumes V_1 and V_2 which significantly exceed the APRS total internal volume. Calculation of pressures $P_{ст}$ and $P_{д}$ was done using the factors obtained at stage 1: dynamic pressure was calculated using formula $P_{д} = qK + KyP_{\infty}$, static pressure – $P_{ст} = KyP_{\infty}$. Supply of pressures $P_{ст}$ and $P_{д}$ in APRS was done simultaneously with operation of a quick-action motor operated valve (QAMOV). Fig. 1, b shows a simplified laboratory bench of APRS.

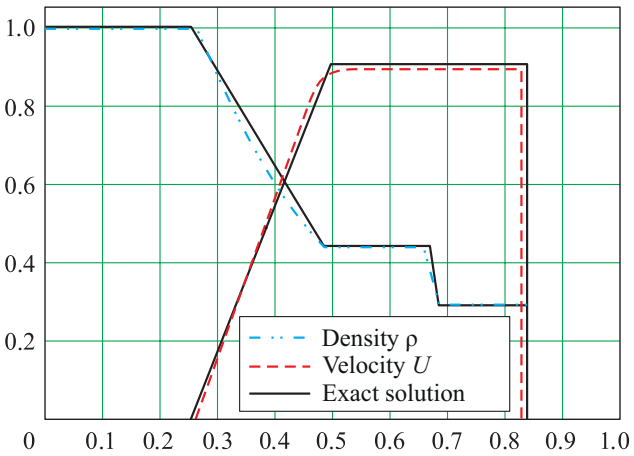

Fig. 4. Task on discontinuity breakup

Stage 4 included numerical calculations to determine time of PMI actuation within the whole RPAM.

The results of PMI actuation in the relative values $t' = t/t_{max}$ and $V' = (V - V_{min})/(V_{max} - V_{min})$ obtained during the LT, laboratory experiments and numerical calculations are given in Fig. 6.

Fig. 6 shows that the results obtained during LT and laboratory experiments correlate well. The results obtained using the SPD computation program and the results of LT and laboratory experiments correlate worse but the correlation is still acceptable. The results are an upper estimate for the PMI actuation time. At this, in all the cases the value of the PMI actuation time has a good margin not exceeding the set value.

Thus, fulfilment of the requirement on the PMI actuation time within the RPAM sub-area without LT are confirmed.

Fig. 6 shows the following: on the abscissa axis $V' = 0…0.322$ – the area of permissible modes of the product operation following

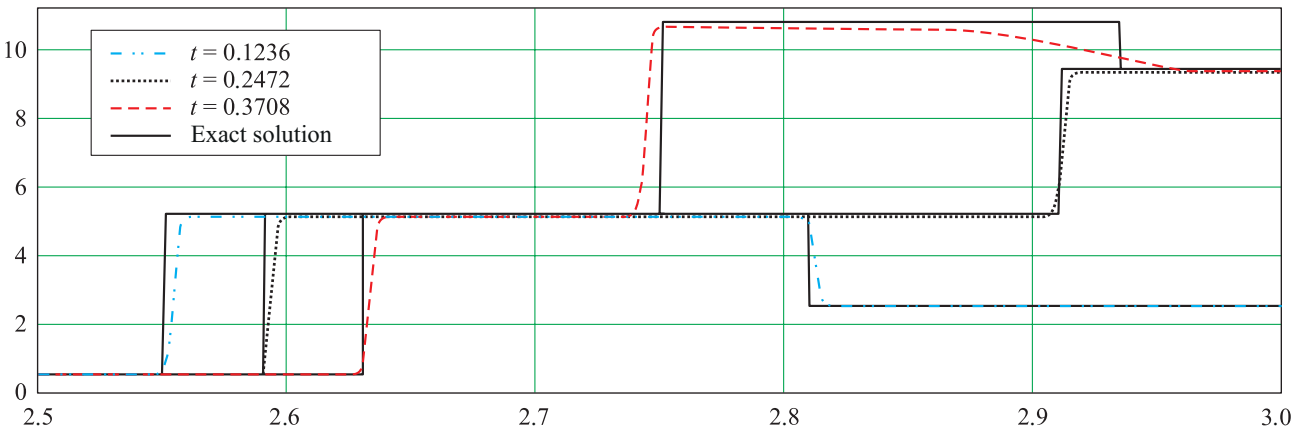

Fig. 5. Task on shock wave reflection from rigid wall

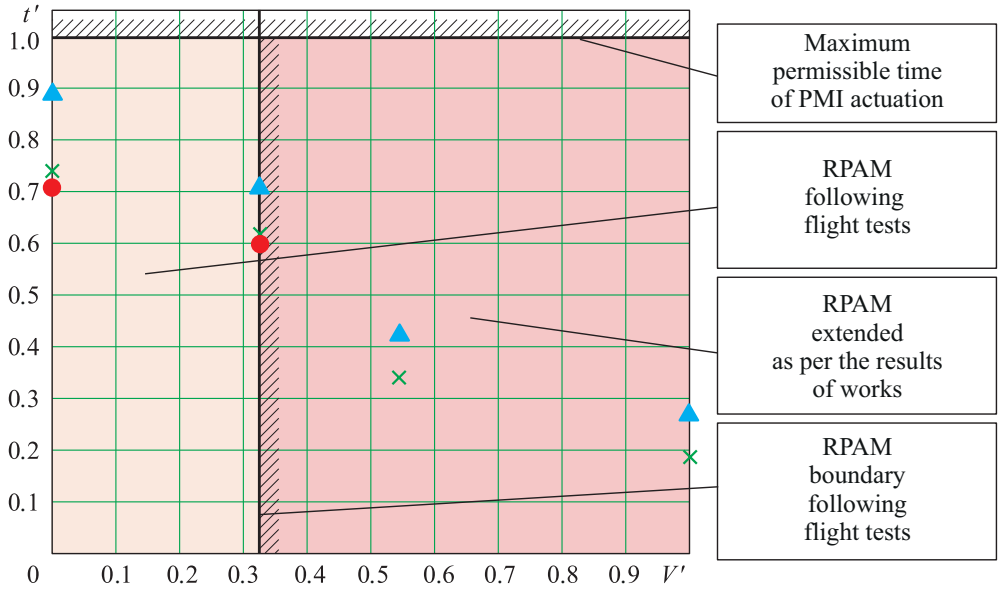

Fig. 6. Scope of product application modes within the coordinates of "dimensionless velocity – dimensionless time of PMI actuation":
● – LT; × – laboratory experiments; ▲ – numerical calculation

the product test flights; on the ordinate axis $t' = 0...1$ – the area of permissible PMI actuation times. Moreover, the area of the product operation modes is shown within the range from $V' > 0.322$ to $V' = 1$; the area was extended following the works done and described herein.

Thus, the use of the approach stated herein allowed significant extension of the aeronautical product permissible operation modes with no additional flight tests.

Bibliography

1. *Brode H. L.* Theoretical description of the performance of the UTIAS hypervelocity launcher // Mekhanika. Novoye v zarubezhnoy nauke. No. 4. M.: Mir, 1976. P. 51–68.

2. *Brode H. L., Shuster S.* Water hammers and safety of boiling water nuclear reactors. Possibility of numerical methods // Mekhanika. Novoye v zarubezhnoy nauke No. 26. M.: Mir, 1981. P. 131–165.

3. *Yanenko N. N.* The method of fractional steps. The solution of problems of mathematical physics in several variables. Novosibirsk: Nauka, 1967. 196 p.

4. Glimm method modification for penetration problems / *S. G. Andreev* [et al.] // Voprosy Atomnoy Nauki i Tekhniki. 1985. Iss. 3. P. 80–85.

5. *Roache P.* Fundamentals of Computational Fluid Dynamics. M.: Mir, 1980. 618 p.

6. *Zamyshlyaev A. A.* Razrabotka matematicheskoy modeli i programmy rascheta protsessa natekaniya sovershennogo gaza v zamknutiy ob'em // Snezhinsk i nauka 2009. Sovremennye problemy atomnoy nauki i tekhniki: Sb. nauch. trudov Mezhdunar. nauch.-prakt. konf. Snezhinsk Chelyabinskoy obl.: Izd-vo SGFTA, 2009. 406 s. (Russian)

Submitted on 23.11.2016

Zamyshlyaev Aleksey Aleksandrovich – Head of Laboratory, Zababakhin All-Russian Scientific Research Institute of Technical Physics, Snezhinsk, Chelyabinsk region.
Science research interests: aerodynamics, ballistics, flight dynamics, aircraft control systems algorithms.

Shmygin Alexandr Nikolaevich – Leading Research Scientist, Zababakhin All-Russian Scientific Research Institute of Technical Physics, Snezhinsk, Chelyabinsk region.
Science research interests: aerodynamics, ballistics, dynamics (hydrodynamics), experimental data processing algorithms.

Donovskiy Dmitry Evgenievich – Candidate of Engineering Sciences, Head of the department, Zababakhin All-Russian Scientific Research Institute of Technical Physics, Snezhinsk, Chelyabinsk region.
Science research interests: aerodynamics, ballistics, flight dynamics, aircraft control systems algorithms.

Исследования с целью расширения области допустимых режимов применения авиационного изделия

Показан цикл расчетно-теоретических и лабораторных работ, проведение которого позволило существенно расширить область режимов применения авиационного изделия без проведения дополнительных летных испытаний. Работы проведены в четыре этапа: определение коэффициентов приема скоростного напора и статического давления, разработка вычислительной программы, проведение лабораторных экспериментов на стенде системы приема воздушного давления и расчетное определение параметров СПВД во всей области режимов применения.

Ключевые слова: коэффициенты приема, область режимов применения, система приема давления, квазиодномерное течение.

Замышляев Алексей Александрович – начальник лаборатории Федерального государственного унитарного предприятия «Российский федеральный ядерный центр – Всероссийский научно-исследовательский институт технической физики имени академика Е. И. Забабахина» (ФГУП «РФЯЦ-ВНИИТФ им. академ. Е. И. Забабахина»), г. Снежинск Челябинской обл.
Область научных интересов: аэродинамика, баллистика, динамика полета, алгоритмы систем управления летательными аппаратами.

Шмыгин Александр Николаевич – ведущий научный сотрудник ФГУП «РФЯЦ-ВНИИТФ им. академ. Е. И. Забабахина», г. Снежинск Челябинской обл.
Область научных интересов: аэродинамика, баллистика, динамика (гидродинамика), алгоритмы обработки экспериментальных данных.

Доновский Дмитрий Евгеньевич – кандидат технических наук, начальник отдела ФГУП «РФЯЦ-ВНИИТФ им. академ. Е. И. Забабахина», г. Снежинск Челябинской обл.
Область научных интересов: аэродинамика, баллистика, динамика полета, алгоритмы систем управления летательными аппаратами.